Journal Name

COMMUNICATION

Pushing the limits of sensitivity and resolution for natural abundance ^{43}Ca NMR using ultra-high magnetic field (35.2 T)

Christian Bonhomme,*[a] Xiaoling Wang,[b] Ivan Hung,[b] Zhehong Gan,[b] Christel Gervais,[a] Capucine Sassoye,[a] Jessica Rimsza,[c] Jingcheng Du,[c] Mark E. Smith,[d] John V. Hanna,[e] Stéphanie Sarda,[f] Pierre Gras,[g] Christèle Combes,[g] and Danielle Laurencin*[h]

Natural abundance ^{43}Ca solid state NMR experiments are reported for the first time at ultra-high magnetic field (35.2 T) on a series of Ca-(pyro)phosphate and Ca-oxalate materials, which are of biological relevance in relation to biominerization processes and the formation of pathological calcifications. The significant gain in both sensitivity and resolution at 35.2 T leads to unprecedented insight into the structure of both crystalline and amorphous phases.

Calcium is an element of major importance, due to its abundance in living organisms and tissues (e.g. bone and teeth), in natural rock-forming minerals (e.g. francolite, calcite, and dolomite), and in major construction materials (e.g. cement, concrete, glass and plaster). However, determining the local environment of this element within complex molecular and materials systems is far from trivial. In particular, structural analysis by ^{43}Ca NMR spectroscopy is highly challenging, due to the poor receptivity of the NMR-active isotope.[1] Calcium-43 is indeed a spin-7/2 quadrupolar nucleus of very low natural abundance (0.14%) and resonance frequency ($v_0(^{43}$Ca) = 57.2 MHz at B_0 = 20 T).

To tackle sensitivity issues, two main approaches have been used in the field of ^{43}Ca solid state NMR.[1-3] The first consists in analyzing large quantities of sample (typically ≥ 300 mg) at high magnetic field (14 to 21 T NMR instruments) under moderate magic angle spinning (MAS) conditions.[1-4] However, even when using signal enhancement NMR sequences for quadrupolar nuclei,[1,5] several hours of acquisition are needed to record a 1D spectrum, which excludes *de facto* the implementation of 2D experiments. Moreover, large quantities of material are not always available, making this approach inapplicable for many systems. The second possibility is to label in ^{43}Ca the compounds of interest.[1,5,6] However, although the gain in sensitivity allows high resolution 1D and 2D correlation experiments to be performed, the major drawback is the high cost of the isotopically-enriched precursor (~ 1500 € for 10 mg of 60% ^{43}Ca-labeled CaCO$_3$). Moreover, it implies that synthetic protocols often have to be re-adapted to start from ^{43}Ca-enriched CaCO$_3$ as a calcium source.

The main challenge today for ^{43}Ca solid state NMR is to find means to reach a much higher sensitivity in order to be able to perform high resolution experiments at natural abundance on a broader variety of materials. In this context, the feasibility of DNP (Dynamic Nuclear Polarization)-enhanced {^{1}H}-^{43}Ca CP (Cross Polarization) MAS experiments at natural abundance was recently demonstrated by Lee *et al* on a 400 MHz instrument (B_0 = 9.4 T).[7] Such DNP analyses are nevertheless constrained by specific experimental features, like the need to find efficient impregnation conditions for each material and to perform measurements at low temperatures. Moreover, the quadrupolar nature of ^{43}Ca actually calls for performing measurements at higher fields to achieve better resolution, because the second-order quadrupolar broadening scales as $1/B_0$. Hence, the possibility of recording natural abundance ^{43}Ca MAS NMR spectra at much higher magnetic fields was investigated. In this article, the first natural abundance ^{43}Ca NMR study at 35.2 T (1.5 GHz ^{1}H Larmor frequency) are reported, using the series-connected hybrid (SCH) magnet at the US National High Magnetic Field Laboratory.[8]

As the SCH magnet is available for a restricted period of time *per day* (~ 7 hours), experiments were first set up by using a ^{43}Ca-labeled monetite sample (*CaHPO$_4$). The radiofrequency

a. *Sorbonne Université, CNRS, Collège de France, Laboratoire de Chimie de la Matière Condensée de Paris, LCMCP, F-75005 Paris, France (CB: christian.bonhomme@upmc.fr)*

b. *National High Magnetic Field Laboratory, 1800 East Paul Dirac Drive, Tallahassee, FL 32310–3706, USA.*

c. *Department of Materials Science and Engineering, University of North Texas, Denton, Texas 76207, USA*

d. *Department of Chemistry, Lancaster University, Lancaster LA1 4YB, UK*

e. *Department of Physics, Warwick University, Coventry, CV4 7AL, UK*

f. *CIRIMAT, Université de Toulouse, CNRS, Université Paul Sabatier, 4 allée E. Monso, 31030 Toulouse cedex 4, France*

g. *CIRIMAT, Université de Toulouse, CNRS, INPT - Ensiacet, 4 allée E. Monso, 31030 Toulouse cedex 4, France*

h. *ICGM, UMR 5253, CNRS-UM-ENSCM, Place E. Bataillon, CC1701, 34095 Montpellier cedex 05, France (DL : danielle.laurencin@umontpellier.fr)*

† Footnotes relating to the title and/or authors should appear here.
Electronic Supplementary Information (ESI) available: [details of any supplementary information available should be included here]. See DOI: 10.1039/x0xx00000x

(RF) power on the ^{43}Ca channel was optimized for best efficiency of the multi-DFS (double frequency sweep) signal enhancement pulse sequence (final gain in signal-to-noise: ~ 2).[5] Moreover, measurements on *CaHPO$_4$ were repeated on different days using a modified/enhanced Bruker lock system, showing no detectable variation in frequency, which demonstrates the reliability of comparisons made on spectra recorded on different days. All NMR experimental parameters (including temperature, MAS probe, pulse schemes, relaxation delays, number of scans and procedure for chemical shift referencing[9]) are given in the Supporting Information.
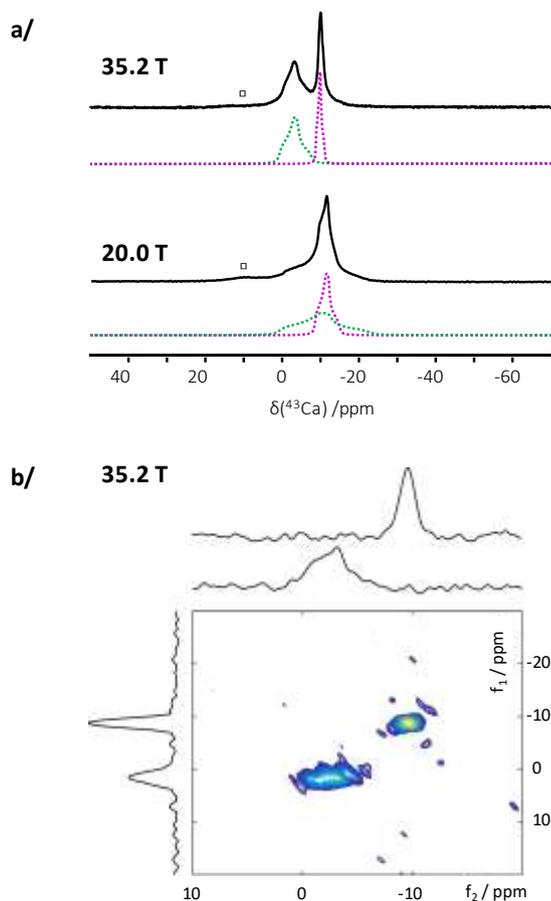

Figure 1 : a/ ^{43}Ca MAS NMR spectra of *CaHPO$_4$ at 20.0 and 35.2 T, together with their fit considering two average Ca environments {δ_{iso}(^{43}Ca) = 0.7 ± 0.8 ppm; |$^{exp}C_Q$(^{43}Ca)| = 3.5 ± 0.3 MHz, $^{exp}\eta_Q$(^{43}Ca) = 0.8 ± 0.1, *and* {δ_{iso}(^{43}Ca) = −8.5 ± 0.8 ppm; |$^{exp}C_Q$(^{43}Ca)| = 1.8 ± 0.3 MHz, $^{exp}\eta_Q$(^{43}Ca) = 0.8 ± 0.1} ($\square$ corresponds to a minor impurity); b/ ^{43}Ca 3QMAS spectrum of *CaHPO$_4$ at 35.2 T.

Measurements on *CaHPO$_4$ illustrate the significant gain *in resolution* which is achieved at 35.2 T (Figure 1a). Indeed, two resonances are clearly resolved at this field, and a second-order quadrupolar lineshape is even observed for the most deshielded signal, which was not the case at lower fields (≤ 20.0 T) due to the strong overlap between resonances. The NMR parameters {δ_{iso}, C$_Q$, η_Q} of the two resonances were extracted by simulations at both fields. Given that the monetite structure actually exhibits 4 different Ca sites, a shifted-echo 3QMAS experiment was performed aiming at further ^{43}Ca resolution.

The 2D spectrum could be recorded in just ~ 50 minutes with a very good signal to noise ratio, due to the significant gain in sensitivity at 35.2 T (Figure 1b). However, only two isotropic chemical shifts were observed in the f1 (indirect) dimension. According to GIPAW-DFT[10] (Gauge Including Projector Augmented Wave - Density Functional Theory) calculations on the monetite structure, this can be explained by the fact that the four inequivalent Ca sites can be divided in two groups exhibiting very similar ^{43}Ca NMR parameters, with the following averaged values:[9] {$^{calc,avg}\delta_{iso}$(^{43}Ca) = 4.2 ppm, $^{calc,avg}C_Q$(^{43}Ca) = −2.3 MHz, $^{calc,avg}\eta_Q$(^{43}Ca) = 0.40} *and* {$^{calc,avg}\delta_{iso}$(^{43}Ca) = −4.4 ppm $^{calc,avg}C_Q$(^{43}Ca) = 1.4 MHz, $^{calc,avg}\eta_Q$(^{43}Ca) = 0.59}. Although this provides an explanation of the observed spectrum, understanding in detail the remaining discrepancy between these calculated average parameters and the experimental ones is still under study, and beyond the scope of the present article. Indeed, careful analyses of both the structural model of monetite and the computational approach used (including the choice of shielding reference, which is difficult to determine accurately) will need to be performed for this.
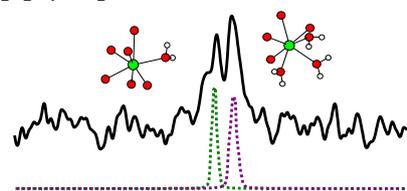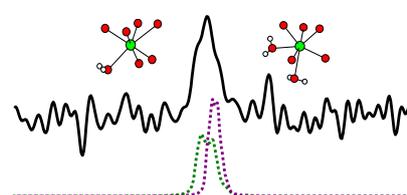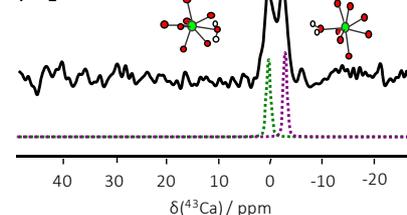
Figure 2: Natural abundance ^{43}Ca MAS NMR spectra of m-Ca$_2$P$_2$O$_7$.4H$_2$O (m-CPPT β, 2.5 hours), t-Ca$_2$P$_2$O$_7$.2H$_2$O (t-CPPD, 3 hours) and CaC$_2$O$_4$.H$_2$O (COM, 3 hours), recorded at 35.2T. The dashed lines show the simulation of the contributions of the two inequivalent Ca-sites in each structure, using the experimental ^{43}Ca NMR parameters determined previously (which are recalled in supporting information in Table S2).[2,3]

With the gains in both sensitivity and resolution at 35.2 T, *natural abundance* ^{43}Ca MAS NMR experiments were carried out on ~30 mg of crystalline calcium pyrophosphate and oxalate compounds (Figure 2). In less than 4 hours, highly

resolved spectra were obtained, while more than 5 hours and larger quantities of sample (~ 300 mg) had been needed previously at 20.0 T to study these phases.[2,3] Most importantly, for monoclinic calcium pyrophosphate tetrahydrate beta (m-$Ca_2P_2O_7$.4H_2O, noted also m-CPPT β) and calcium oxalate monohydrate (CaC_2O_4.H_2O, noted also COM), for which the two crystallographic Ca sites were barely resolved at 20.0 T (the isotropic chemical shifts being separated by less than 3.5 ppm),[2,3] clear resolution was achieved at 35.2 T. In contrast, for the triclinic calcium pyrophosphate dihydrate phase (t-$Ca_2P_2O_7$.2H_2O, noted also t-CPPD), in which the ^{43}Ca isotropic shifts are separated by less than 2.5 ppm and the quadrupolar coupling constants are slightly larger ($|C_Q| \sim 3$ MHz), the two sites are not resolved. More generally, for ^{43}Ca sites characterized by $C_Q(^{43}Ca) \leq 3$ MHz, second-order quadrupolar broadening effects are almost absent at 35.2 T, and the breadth of the signals is hence a reflection of the distribution in isotropic chemical shifts and/or the intrinsic relaxation of ^{43}Ca. This is obviously the case for the COM sample (Figure 2).

Based on the encouraging measurements made on the crystalline Ca-pyrophosphate and oxalate phases (Figure 2), the characterization of an *amorphous* pyrophosphate phase $Ca_2P_2O_7$.xH_2O (a-CPP, x ~ 4) at 35.2 T was undertaken. This sample represented a much greater challenge for natural abundance ^{43}Ca NMR, due to wider range of variation of the chemical shift and quadrupolar NMR parameters, which lead to broader signals.[2] Moreover, given that Ca-sites with large quadrupolar coupling constants ($|C_Q(^{43}Ca)| > 5.5$ MHz) can be found in amorphous materials,[11] natural abundance ^{43}Ca MAS NMR measurements at "lower" fields ($B_0 \leq 20$ T) using spinning speeds of ~ 5 kHz (which is in practice the upper limit for some of the commercial large volume rotors) could actually lead to misleading lineshapes. As a matter of fact, very few data related to calcium containing glasses (labeled in ^{43}Ca),[12,13] and amorphous derivatives (in natural abundance) have been published so far.[1,2]

The natural abundance ^{43}Ca MAS NMR spectrum of a-CPP was recorded at 35.2 T (Figure 3a). Thanks to the very fast relaxation of ^{43}Ca in the sample, less than 4 hours were needed to record the spectrum, which is all the more remarkable when considering that the signal is ~ 10 times broader in comparison to those of the crystalline phases reported above.

In order to gain greater 'chemical insight' into the origin of these distributions, computational models of the amorphous compound were developed, using Monte Carlo (MC) based simulations with bond constraints followed by relaxation with Ab-Initio Molecular Dynamics (AIMD) simulations and geometry optimization with DFT calculations (see supporting information). It should be noted that in contrast to non-hydrated calcium derived glasses,[13] the commonly used melt-quench approach for MD could not be used to model amorphous $Ca_2P_2O_7$.4H_2O, as it would have led to condensed phosphate chains with various lengths and would not have been able to tackle the presence of water molecules. Here, using combined MC, AIMD, and DFT calculations, three models of this amorphous phase with hydrated calcium pyrophosphate groups were generated (each with 12 Ca sites, see Figure 3b).[§] For each

model, calculated Pair Distribution Function (PDF) analyses were compared to the experimental data, showing that the agreement is reasonable (Figure S3 in supporting information).
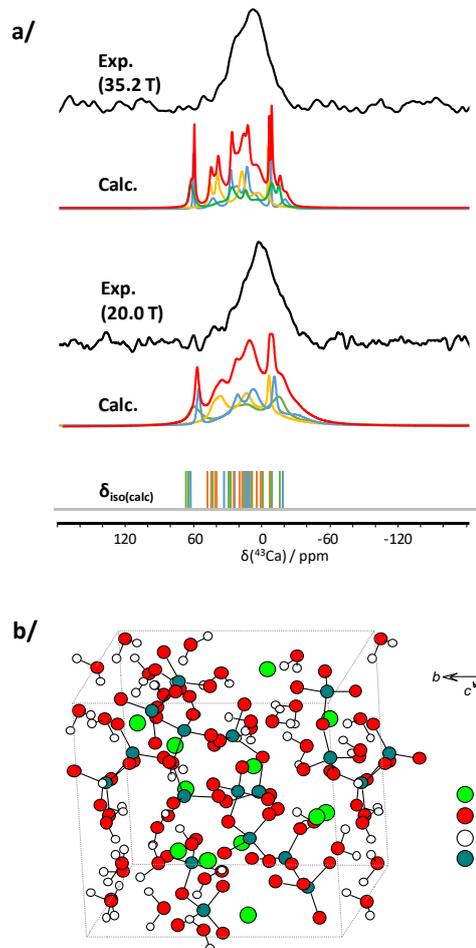

Figure 3: a/ ^{43}Ca MAS NMR spectra of amorphous-$Ca_2P_2O_7$.4H_2O (a-CPP) at 20.0 and 35.2 T, together with the GIPAW-DFT ^{43}Ca NMR calculations related to the three AIMD derived models (sum in red, contributions of Models I, II and III in blue, orange and green respectively; calculated isotropic shifts are shown as vertical bars); b/ AIMD derived computational model of a-CPP (Model I) used for DFT calculations (see supporting information for further details as each of three models provides 12 calcium sites).

The analysis of the Ca local environments in these models demonstrates that *(i)* coordination numbers range between 4 and 9, *(ii)* up to 5 water molecules can be bound to Ca^{2+}, and *(iii)* the average Ca…O bond distances are between 2.3 and 2.6 Å (see Supporting Information, Table S4). These values are in agreement with the structural parameters of the crystalline calcium pyrophosphate phases (dihydrate and tetrahydrate). Coordination numbers range from 6 to 7 for calcium atoms in these structures and bond distances are between 2.257 and 2.668 Å.[14-16] DFT calculations of the ^{43}Ca NMR parameters were then carried out, using the GIPAW-DFT approach (see Supporting Information for computational details). The range of variation of the calculated isotropic chemical shift (-16.1 ppm < $^{calc}\delta_{iso}(^{43}Ca)$ < 64.3 ppm; average value of 21.6 ppm) and quadrupolar coupling constants (1.2 MHz < $|^{calc}C_Q(^{43}Ca)|$ < 6.5 MHz; average value of 3.4 MHz) is consistent with the

experimental data (Figure 3a). More specifically, it is worth noting that the calculated values $^{calc}\delta_{iso}(^{43}Ca)$ spread out across the experimental lineshape obtained at 35.2 T, with more of the calculated values positioned where the signal has maximum intensity. Despite the lack of sufficient statistics at this stage, which are visible from the simulated sums of the models (Figure 3a, red curves), these AIMD models appear as the first realistic starting point for describing Ca local environments in these amorphous materials. In Figure S4, additional simulations including Czjzek distributions of quadrupolar parameters (Gaussian Isotropic Model, GIM) as well as Gaussian distributions of ^{43}Ca isotropic chemical shifts[17] are presented, which show that at ultra-high magnetic field, it is likely that simple distributions of isotropic chemical shifts are mainly observed. Finally, it should be noted that GIPAW NMR calculations were performed at 0K, therefore not taking into account potential local dynamics of the water molecules,[2] which could affect the ^{43}Ca NMR parameters. Low temperature ^{43}Ca NMR experiments will need to be performed in the future to investigate this aspect.

All in all, the 1.5 GHz series connected hybrid instrument paves new avenues for natural abundance ^{43}Ca MAS NMR. Significant gains in both resolution and sensitivity were demonstrated in the case of crystalline calcium pyrophosphate and oxalate phases. Most importantly, thanks to favorable relaxation characteristics, the natural abundance ^{43}Ca MAS NMR spectrum of an amorphous hydrated calcium pyrophosphate was successfully obtained, which could be compared for the first time to computational models of this phase. This point is of crucial importance as amorphous precursors of calcium carbonate,[18] calcium oxalate[19] and calcium (pyro)phosphates[20] are meant to play a fundamental role in biomineralization processes, which have not been fully characterized so far (notably regarding Ca environments). Moreover, such ^{43}Ca NMR experiments at ultra-high magnetic field may also provide complementary clues regarding the *polyamorphism* of biomaterials.[2,21]

Conflicts of interest

There are no conflicts to declare.

Notes and references

1   C. M. Widdifield, *Ann. Rep. NMR Spectrosc*, 2017, **92**, 227; D. Laurencin and M.E. Smith, *Prog. Nucl. Magn. Res. Spectrosc.* 2013, **68**, 1; D. Bryce, *Dalton Trans* 2010, **39**, 8593.
2   P. Gras, A. Baker, C. Combes, C. Rey, S. Sarda, A. J. Wright, M. E. Smith, J. V. Hanna, C. Gervais, D. Laurencin and C. Bonhomme, *Acta Biomater.* 2016, **31**, 348.
3   H. Colas, L. Bonhomme-Coury, C. Coelho Diogo, F. Tielens, F. Babonneau, C. Gervais, D. Bazin, D. Laurencin, M. E. Smith, J. V. Hanna, M. Daudon and C. Bonhomme, *CrystEngComm*, 2013, **15**, 8840.
4   S. Chen, B. E. G. Lucier, M. Chen, V. V. Terskikh, Y. Huang *Chem. Eur. J.* 2018, **24**, 8732.
5   K. M. N. Burgess, F. A. Perras, I. L. Moudrakovski, Y. Xu, and D. L. Bryce, *Can. J. Chem.* 2015, **93**.
6   D. Laurencin, A. Wong, J. V. Hanna, R. Dupree and M. E. Smith, *J. Am. Chem. Soc.* 2008, **130**, 2412; A. Wong, D. Laurencin, R. Dupree and M. E. Smith, *Sol. St. Nucl. Magn. Res.* 2009, **35**, 32; D. Laurencin, C. Gervais, A. Wong, C. Coelho, F. Mauri, D. Massiot, M. E. Smith and C. Bonhomme, *J. Am. Chem. Soc.* 2009, **131**, 13430.
7   D. Lee, C. Leroy, C. Crevant, L. Bonhomme-Coury, F. Babonneau, D. Laurencin, C. Bonhomme and G. De Paëpe, *Nature Comm.* 2017, **8**, 14104.
8   Z. Gan, I. Hung, X. L. Wang, J. Paulino, G. Wu, I. M. Litvak, P. L. Gor'kov, W. W. Brey, P. Lendi, J. L. Schiano, M. D. Bird, L. R. Dixon, J. Toth, G. S. Boebinger and T. A. Cross, *J. Magn. Reson.* 2017, **284**, 125.
9   C. Gervais, D. Laurencin, A. Wong, F. Pourpoint, J. Labram, B. Woodward, A. P. Howes, K. J. Pike, R. Dupree, F. Mauri, C. Bonhomme and M. E. Smith, *Chem. Phys. Lett.* 2008, **464**, 42.
10 C. J. Pickard and F. Mauri, *Phys Rev B*, 2001, **63**, 245101.
11 A. Pedone, T. Charpentier and M. C. Menziania, *Phys. Chem. Chem. Phys.* 2010, **12**, 6054.
12 K. Shimoda, Y. Tobu, Y. Shimoikeda, T. Nemoto and K. Saito, *J. Magn. Reson.* 2007, **186**, 156; F. Angeli, M. Gaillard, P. Jollivet and T. Charpentier, *Chem. Phys. Lett.* 2007, **440**,324.
13 E. Gambuzzi, A. Pedone, M. C. Menziani, F. Angeli, P. Florian, T. Charpentier, *Solid St. Nucl. Magn. Reson*. 2015, **68-69**, 31.
14 N. S. Mandel, *Acta Cryst. B* 1975, **31**, 1730.
15 T. Balić-Žunić, M. R. Christoffersen and J. Christoffersen, *Acta Cryst. B* 2000, **56**, 953.
16 P. Gras, C. Rey, G. André, C. Charvillat, S. Sarda and C. Combes, *Acta Cryst. B* 2016, **72**, 96.
17 D.R. Neuville, L. Cormier and D. Massiot, *Geochim. Cosmochim. Acta* 2004, **68**, 5071.
18 Y. Wang, S. Von Euw, F.M. Fernandes, S. Cassaignon, M. Selmane, G. Laurent, G. Pehau-Arnaudet, C. Coelho, L. Bonhomme-Coury, M.-M. Giraud-Guille, F. Babonneau, T. Azaïs, N. Nassif, *Nature Mater*., 2013, **12**, 1144; S. Weiner, Y. Levi-Kalisman, S. Raz and L. Addadi, *Connect Tissue Res*. 2003, **44**, 24.
19 E. Ruiz-Agudo, A. Burgos-Cara, C. Ruiz-Agudo, A. Ibanez-Velasco, H. Cölfen and C. Rodriguez-Navarro, *Nature Commun*. 2017, **8**, article 768.
20 K. Ley-Ngardigal, C. Combes, S. Teychene, C .Bonhomme, C. Coelho-Diogo, P. Gras, C. Rey and B. Biscans, *Cryst. Growth & Design*, 2017, **17**, 37.
21 J.H.E. Cartwright, A.G. Checa, J.D. Gale, D. Gebauer and C.I. Sainz-Diaz, *Angew. Chem*. 2012, **51**, 11960.